DETECTION OF EXUDATES FROM DIGITAL FUNDUS IMAGES USING A REGION-BASED SEGMENTATION TECHNIQUE

Hussain F. Jaafar, Asoke K. Nandi and Waleed Al-Nuaimy

Department of Electrical Engineering and Electronics
University of Liverpool, Brownlow Hill, Liverpool, L69 3GJ, UK
fax: +44 151 794 4540, email: {h.jaafar, a.nandi, wax}@liverpool.ac.uk, web: www.liv.ac.uk

ABSTRACT

The detection and quantification of exudates can contribute to the mass screening of the diabetic retinopathy, the major cause of blindness. In this work, we outline detection techniques of the main retinal structures, namely the blood vessels, optic disk and fovea. A new method for the detection of exudates using adaptive thresholding and classification is proposed in which the retinal structures are used to remove artefacts from exudate detection results. The proposed adaptive thresholding proceeds through two stages: (1) image decomposition into a number of homogeneous sub-images using a region-based segmentation technique, and (2) edge detection using a morphological gradient technique. Classifying the exudates from non-exudates was carried out using rule-based classification. Using a clinician reference (ground truth), the proposed method was validated, in terms of pixels, with overall sensitivity of 93.1%. Speed and performance of the proposed method show that it is more reproducible than the manual method.

Index Terms— Medical imaging, retinal structures, exudate detection, region-based segmentation, edge detection.

1. INTRODUCTION

Diabetic retinopathy (DR), the major cause of poor vision, is an eye disease that is associated with long-standing diabetes. If the disease is detected in its early stages, treatment can slow down the progression of DR. However, this is not an easy task, as DR often has no early warning signs. Earliest signs of DR are damages to the blood vessels and then the formation of lesions. Lesions such as exudates are normally detected and graded manually by clinicians in time-consuming and is susceptible to observer error. A computer-aided detection of exudates could offer fast and precise diagnosis to specialist inspection and then will assist the clinician to take timely the right treatment decision.

Several methods for the detection of exudates have been reported in the literature [1]-[6]. In Reza *et al.* [1], the bright objects such as optic disk and exudates were detected based on marker-controlled watershed segmentation and making use of average filtering and contrast adjustment. The fuzzy C-means clustering was used by Sopharak *et al.* [2] for the segmentation of exudates followed by classification using a morphological technique. In Garcia *et al.* [3] a combination of local and global thresholding was used to segment exudates followed by investigating three neural network classifiers to classify exudates. A method based on mathematical morphology for exudate detection has been proposed by Welfer *et al.* [4]. In Sanchez *et al.* [5] a method based on mixture models has been proposed to separate exudate from background followed by edge detection technique to distinguish hard exudates from soft exudates. Li *et al.* [6] proposed a method based on dividing the image into 64 sub-images followed by applying a combination of region growing and edge detection to detect exudates.

In this paper, novel methods for extraction of retinal structures and exudate detection are presented. The novelty of our work is attributed to the exploitation of geometric relations among retinal structures to extract them and using a combination of region-based segmentation and edge detection techniques for the detection of exudates. Details of the proposed methods are presented in Section 2. The results and discussions are presented in Section 3. Section 4 presents our conclusions and future work.

2. METHODOLOGY

Fig. 1 presents a block diagram outlining proposed methods to automated extraction of retinal structures and automated detection of exudates from retinal images.

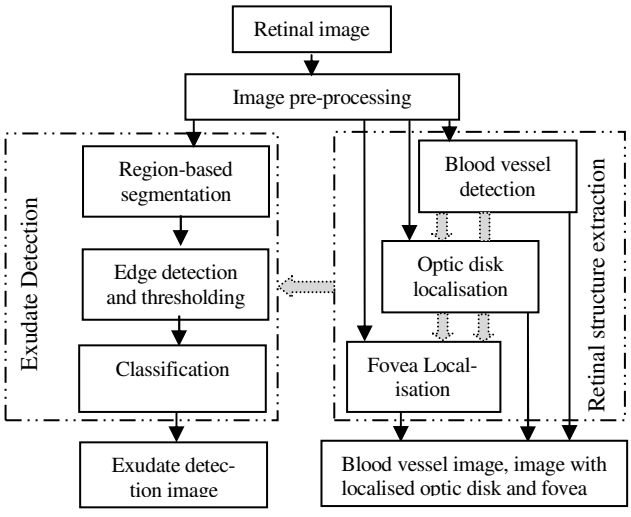

Fig.1 A block diagram outlining the proposed method steps.

2.1 Pre-processing

Most retinal images are non-uniform illuminated and sometimes have low visual contrast. Pre-processing steps, namely shade correction and contrast enhancement, were carried out to prepare the image for next processing with better quality.

2.1.1 Shade correction

To correct non-uniform illumination of the image, a morphological top-hat operation was used. Top-hat operation is based on producing a reasonable estimate of the background across the green channel of the original image using morphological opening and closing operations with a large structuring element enough to avoid entirely fitting within small candidate regions. To avoid unexpected bright areas at the borders and around the bright optic disk, we used, in the estimation process, alternating sequential opening and closing with a disk-shaped structuring element of a fixed radius of 3 pixels and 8 alternative repetitions between opening and closing. The estimated background is then subtracted from the green channel component to produce a shade corrected image. Effectiveness of the shade correction operation relies dramatically on the non-uniformity grade of the image and the size selection for the structuring element.

2.1.2 Contrast enhancement

The retinal images are sometimes poorly contrasted; thus, the retinal structures and exudates are not easily distinguishable from the background. Consequently, a processing of contrast enhancement is vital to improve the contrast of the image. For this, a Contrast-Limited Adaptive Histogram Equalization (CLAHE) was applied to the intensity channel of the image after conversion from the RGB to HSI colour space. The HSI colour space is appropriate since the intensity component is separated from the other two components. CLAHE enhances the image by transforming the intensity values of the image. It operates on small regions instead of the entire image. The contrast of each small region is enhanced with histogram equalization. The resulting HSI components are converted again to RGB space to achieve the pre-processed image from the green channel component image, shown in Fig. 2(a). The pre-processed image is shown in Fig. 2(b).

2.2 Extraction of Retinal Structures

Features of retinal structures are widely used in diagnosing many eye diseases, such as DR, glaucoma, age-related macular degeneration and others. Moreover, they have a significant importance in following up the evolution of lesions over time. But, these structures mostly appear similar to characteristic features of bright and red lesions. Therefore, most artefacts, which affect the performance of DR detection, are created due to contrasted retinal structures. Hence, the detection of retinal structures is important to test retinal health state and to fine-tune exudate detection results as well.

2.2.1 Detection of the blood vessels

Retinal blood vessels appear with many observable features such as diameter, colour and orientation. These features may change due to some diseases, such as diabetes mellitus, hypertension and retinopathy of prematurity.

In this paper, we propose a simple and computationally fast method to detect retinal blood vessels by applying a morphological closing operator to the pre-processed image two times with two different scales of disk-shaped structuring elements. The radius of the larger disk is 8 pixels and the smaller one is 2 pixels, knowing that these values are compatible with image size of 640×480 pixels. Then the closed image with the smaller structuring element is subtracted from the larger one followed by thresholding to obtain initial binary image of the blood vessels. After many experiments we found that the appropriate threshold value is about 90% of the maximal intensity.

With variable image conditions (normal or abnormal) and qualities (uniform or non-uniform illuminated), the initial blood vessel image may include other type of dark regions with variable shapes and sizes. Discrimination of the blood vessels from other dark regions could be accomplished using a rule-based classifier. The rules, in our work, are empirically derived from the data of training by a series of comparison between many pairs of features and looking for functions of every two features. The selected features are: length, width, area, perimeter, eccentricity, circularity, average intensity and whole intensity. Short breaks in detected vessel lines could be connected using smoothing splines. A final blood vessels image is illustrated in Fig. 2(c).

2.2.2 Localisation of the optic disk

The optic disk (OD) is the intraocular part of the optic nerve formed by fibers and appearing as a pink to white disk. Information of the OD is widely used to examine some diseases such as glaucoma. Moreover, its location and size are important issue in retinal image analysis, for example as a reference to measure distances and then identify other anatomical parts in the retinal image, e.g. the fovea.

In this paper, we followed and implemented a method described in [7], where the mathematical morphology, particularly dilation and erosion operators, is used for analysing shapes in the image. The binary image is computed from the pre-processed image by the area thresholding method. The initial boundary of the optic disc is traced from that binary image. Then, a circular region of interest, from the initially traced blob boundary, is used to find the contour of the OD. The magnitude gradient of the image for the region of interest is computed using closing operator to fill the vessels followed by opening operator to remove large peaks. A morphological basic gradient is calculated by subtracting the eroded image from the dilated image. The boundary and the centre of the OD are determined by applying the Hough transform to the gradient image. A result of OD detection is illustrated in Fig. 2(f).

2.2.3 Localisation of the fovea

The fovea is the part of the eye that is responsible for central vision which is necessary in humans for all activities where visual detail is required. Hence, determining the location of the fovea is essential to evaluate the severity of lesions. Localisation of the fovea has been proposed by many researchers such as Sekhar *et al.* [8] and Li *et al.* [6]. In this paper, we propose a method based on the combination of the attributes of both methods in [8] and [6] to localise the fovea with a better performance.

The fovea is the darkest part in the retinal image and located in the centre of the macula region where no blood vessels. The two main retinal blood vessels, which together are

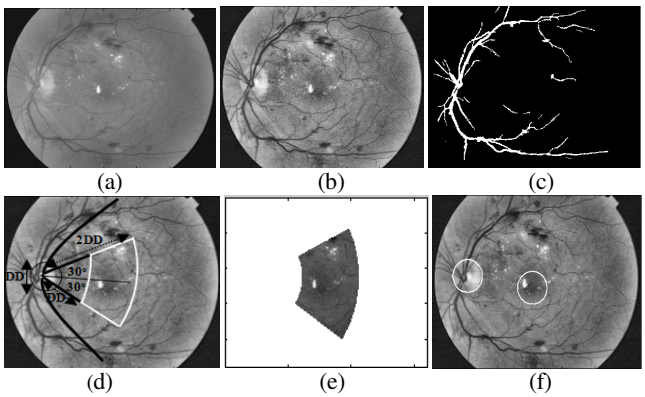

Fig. 2 – Input and results of both pre-processing and retinal structures extraction. (a) A green channel image. (b) A pre-processed image. (c) A blood vessel image. (d) Geometry of fovea candidate. (e) ROI for locating fovea. (f) Image with localised OD and fovea.

parabolic-like shape, have, in the majority of retinal images, similar geometric relation with the fovea. Hence, they are fitted as a parabola with a vertex location on the centre of the OD. The main courses of blood vessels can be fitted to parabola using a clustering, such as Hough transform to map the data into quantized parameter space [6].

A candidate region of interest is defined as the part of sector subtended to the OD by an angle of 30^{o} above and below the parabola axis [8]. The angle value is selected so as to circumscribe within the sector part a circle of two times the diameter of OD. Within the selected candidate region, the threshold value is calculated in such a way that the value in which the segmented area has about the same area of OD. This description is shown in the Fig. 2(d) and Fig. 2(e) and the fovea localisation result is illustrated in Fig. 2(f).

2.3 Exudate Detection

Exudates appear as bright regions with different shapes, locations and brightness among different patients. Additionally, the brightness of some exudates may be lower than those of other exudates in the same image. Hence, we conclude that there is no prior knowledge about the shape, location, and brightness of exudates. Exudates are mostly characterized by having distinct borders; while non-exudates, especially those are created due to light reflection, do not have clear boundaries. In this study we focus our attention on three tasks for the detection of exudates as below:

- Rectifying the defect of non-uniform illumination by using a region-based segmentation.
- Exploiting the characteristic of having distinct borders to detect exudates using a morphological gradient.
- Classifying exudates from non-exudates using rule-based classification.

2.3.1 Region-based segmentation

Even after the operation of pre-processing, most of retinal images may not be sufficiently uniform illuminated for global thresholding. With such concern, a region-based segmentation can offer a suitable solution by splitting the image into a number of homogeneous sub-images before the global thresholding. A novel region-based segmentation using a new split-and-merge algorithm has been proposed in our previous work [9]. In the current paper, for the sake of getting attributes of better performance and faster computation, we have used a pure-splitting method rather than the split-and-merge method to avoid the drawback of time-consuming caused by merging operations. In the proposed method the image is successively partitioned into four quadrants to achieve homogeneous sub-images based on predefined criteria. In this stage, we used the pre-processed image (G) after removing the detected OD. For this, an OD mask (O_d) is used to mask its OD location on the pre-processed image by a colour equal to the average intensity of the pre-processed image (I_{av}) to get a new image (G_1), shown in Fig. 3(a), as follows:

$$G_1(i,j) = \begin{cases} I_{av} & if\ O_d = 1 \\ G(i,j) & Otherwise \end{cases}$$

The end of successive partitioning relies on two factors: the homogeneity test and a predefined smallest size. This size must follow threshold (ε) to avoid over-partitioning and then complex computation, where ε is dynamically calculated based on the statistical information of the whole image G_1, namely the mean and the standard deviation. For homogeneity test, we followed a method based on features analysis, described by Chen *et al.* [10]. In this method, a histogram analysis is used for analysing the characteristics of regions and mapping the frequencies of the desired features like gray level distribution and local texture measure.

2.3.2 Edge detection

After image partitioning, the segmentation of exudates was carried out on each sub-image using a morphological gradient where three kinds namely, basic, internal, and external were investigated. The basic gradient is calculated by subtracting the eroded image (acts like a local minimum operator) from the dilated image (acts like a local maximum operator), the internal gradient is calculated by subtracting the eroded image from the original image and the external gradient is calculated by subtracting the original image from the dilated image. Experimental tests for the three gradient kinds showed that the best balance in performance measures, particularly between sensitivity and PPV, could be achieved with the basic gradient. To segment edges from the background as an initial exudate image, a histogram-based thresholding with automatic level (α) was applied to each individual sub-image followed by merging the binary results of all the sub-images. Let a partition (Q) of the image is defined as a subset of G_1 with respect to uniform illumination criterion. Hence running a global thresholding (T) on all the sub-images can be denoted by G_2 as follows:

$$G_2 = \sum_{l \epsilon k} T_\alpha(Q_l)$$

where k is the number of the sub-images. The result of initial exudate detection is illustrated in Fig. 3(b).

2.3.3 Classification

Due to light reflection areas and bright regions between contrasted blood vessels and around the OD, the initial exudate detection image mostly contains some spurious-exudates with variable shapes, sizes, and locations. Hence, based on many experimental tests on abnormal images, a number of

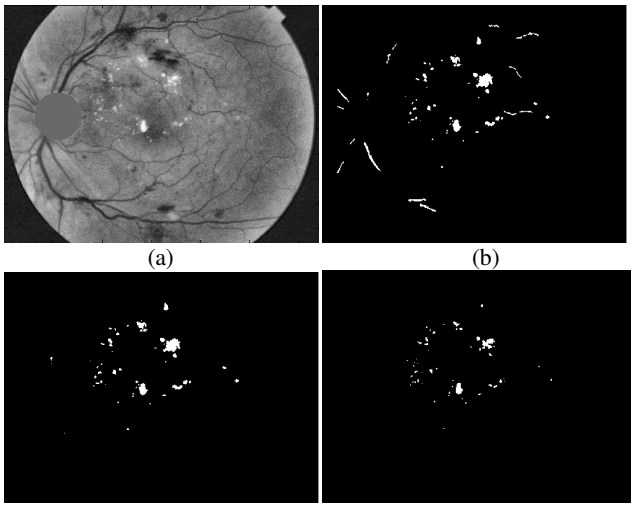

Fig. 3 – Input and results of exudate detection stages. (a) A pre-processed image after masking the OD. (b) The result of region-based segmentation, edge detection and thresholding. (c) The result of (b) after the classification. (d) A clinician hand-labelled image.

rules were assigned in the rule-based classifier to classify the segmented candidates into exudates and non-exudates.

Since the exudates are lipid leaks from the side of swelling tiny blood vessels, they tend to have spherical shape with diameters greater than feeding blood vessels. However, some exudates are elliptical or slightly elongated, so these slight deviations should be tolerated in the lower limits of the criteria The features, aspect-ratio (ratio of major axis length (MJL) to minor axis length(MNL)), area (A), circularity (measure of roundness using area and perimeter (P)) and eccentricity(E) were used as measures of the binary candidate shape. We found empirically that a candidate can be classified as exudate only if its aspect-ratio is less than 1.8, eccentricity is greater than 0.7, circularity is bigger than 0.5 and the area is bigger than 20. Let $Y = Y_1, \dots Y_n$ be a finite set of white regions from the initial exudate image. The image (G_3) without spurious-exudates can be expressed as follows:

$$G_3(i,j) = \begin{cases} G_2(i,j) \;\; if \; \big(MJL(Y_l) < 1.8MNL(Y_l)\big) \wedge \\ \qquad\qquad (E(Y_l) > 0.7) \wedge (4\pi A > 0.5P^2) \\ \qquad\qquad \wedge (A(Y_l) > 20), \qquad l = 1, \dots n \\ 0 \qquad\qquad\qquad\qquad\qquad\qquad Otherwise \end{cases}$$

To make sure of removing any residual vasculature trace from the exudate detection image the blood vessels image is subtracted from the image $G_3$to achieve the final exudate detection image as shown in Fig. 3(c). For visual comparison, the clinician hand-labeled image is shown in Fig. 3(d).

3. MATERIALS, RESULTS AND DISCUSSIONS

The proposed method was trained and tuned on 130 retinal images of which 110 images contain different signs of DR, from the DIARETDB0 database [11]. A set of labelled images reported by experts are provided with this database as a description of visual appearance. Satisfactory evaluation can be achieved when the test images are from other source than training images source. Hence, another 106 retinal images with their ground truth (89 images, of which 47 images contain exudates, from the DIARETDB1 database [12] and 17 retinal images, all of them contain exudates, from the Messidor database [13]) were used to test the proposed method. The overall performance, in pixel-based accuracy, was evaluated using 64 images (of which 47 came from DIARETDB1 database and 17 came from MESSIDOR database). The proposed method found to achieve 93.1% sensitivity, 99.2% specificity, 99.3% accuracy and 78.5% positive predictive value (PPV). To evaluate the proposed method, in image-based accuracy, 89 images from DIARETDB1 were used to achieve 98.9% sensitivity and 91.0% specificity.

Due to lack of a database with their ground truth for retinal structures, the detection of retinal structures were evaluated based on our findings of 89 images, from DIARETDB1, with regard to an expert. We achieved an average sensitivity of 85% and specificity of 90% for the blood vessels detection and a success rate of 100% and 97.8% for the fovea and optic disk localisation respectively.

The disparity between the practical detection results and the ideal results (ground truth) can be used to enhance the performance of the algorithm. Consequently, many experiments have been carried out with an intervention on the automatic threshold α with 12 change rates in both directions (increase and decrease) for each of the three gradient kinds. From these experiments, there appeared to be noticeable influence of a change in α on the balance of performance measures with different manner for each gradient kind as illustrated in the Fig. 4. In these experiments, we focused our attention only on the sensitivity and PPV, in pixel-based accuracy, because they are the most meaningful performance among the other performance measures.

From a prior knowledge about the performances of many previous works, we estimate a least reasonable performance for the sensitivity as 80% and the PPV as 65%. From looking at the parts of the ROC curves delimited by estimated least values and greater values, we conclude that the basic gradient can detect exudates with a sensitivity clearly better than those of the other kinds, while the internal gradient can detect exudates with PPV noticeably better than that of the basic gradient and much better than that of the internal gradient. The reason for this is that the basic gradient operator detects all regions between outer dilated edges and misses small inner regions and hence leads to include most wanted true positives (TPs) (enhances the sensitivity) and some undesired false positives (FPs) (affects the PPV). While in case of internal gradient operator, because it uses the original image (without dilation), some TPs will be missed and at the same time it will get a benefit of getting rid of some FPs that leads to enhance the PPV. In external gradient, the resulting image suffers from missing many TPs and containing more FPs which affects both sensitivity and PPV. However, the selection of appropriate change rate in the α, within the range of least reasonable performance onwards, and the kind of the gradient, will then depend on the medical diagnosis requirements and can be decided by the clinician.

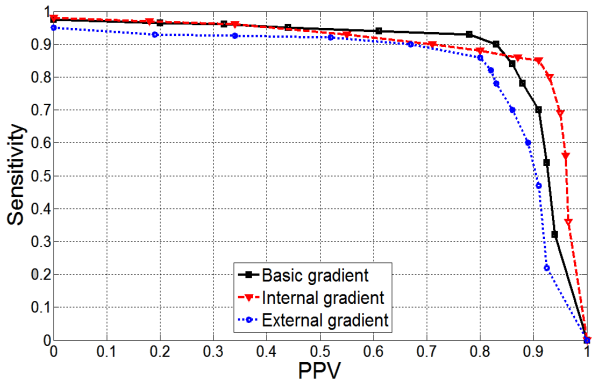

Fig. 4 – ROC curves of α influence on the balance between the sensitivity and PPV for the three morphological gradient kinds.

Table 1 Comparison of performance measures for the proposed method and other previous related works.

Method	Test set	Pixel-based		Image-based	
		SE%	PPV%	SE%	SP%
Sopharak [2]	40	87.3	42.8	-	-
Garcia [3]	67	87.6	83.5	100	77.8
Sanchez [5]	80	90.2	96.8	100	90
Li [6]	35	-	-	100	71
Walter [13]	15	92.8	92.4	100	86.7
Prpsd mthd	106	93.1	78.5	98.9	91

Prpsd mthd = Proposed method, SE = Sensitivity, SP = Specificity.

To evaluate the performance of the proposed method, a comparison of performances of the proposed method with other existing recent works is summarised in Table 1. This table shows that the proposed method detected exudates with distinctive sensitivity, in pixel level calculation, and distinctive specificity, in image-based classification compared with the other works. Although the PPV value of the proposed method does not reach to those, reported in some other works, the comparison should be made with considering other attributes of the proposed method notably its ability to deal with a variety of image quality. This attribute are acquired by using the technique of region-based segmentation in which the image is dynamically divided into homogeneous sub-images. This technique is also used by Li *et al.* [6] but with a fixed number of image dividing which leads to relatively slow computation speed. A low PPV interprets a high level of FPs. Anyhow, this does not, in our case, result in false alarms because FPs tend to lie in the immediate vicinity of TPs (in between small blobs), then resulting interpretation of images is unaffected.

4. CONCLUSIONS

In this paper, we outline novel methods for automated detection of the retinal structures and exudates from retinal images. In the detection of retinal structures, we made use of geometric relations among them in addition to their individual specifications. In the detection of exudates, we have exploited the attribute of having clear boundaries using a morphological gradient technique to discriminate exudates from other bright non-exudate objects. Additionally, a technique of pure splitting was used to decompose the image into homogeneous sub-images to achieve an efficient detection for variant image quality. Disparities between the proposed method results and the ground truth were investigated using an intervention on the automatic threshold α for each of the three gradient kinds to study its influence on the performance measures of each gradient kind. Despite its superior performance and the ability to deal with variant image quality, the proposed method still needs to be expanded to include all signs of DR. Hence, our future work will undertake detecting the other types of lesions associated with DR.

5. ACKNOWLEDGEMENTS

The authors would like to thank the DIARETDB0 Database Centre [11], the DIARETDB1 Database centre [12] and the Centre of Mathematical Morphology, Mines Paris Tech. [13] for their cooperation in providing retinal images. Hussain F. Jaafar would like to acknowledge the financial support of the Iraqi government.

REFERENCES

[1] A. W. Reza, C. Eswaran and K, Dimyati, "Diagnosis of Diabetic Retinopathy: Automatic Extraction of Optic Disc and Exudates from Retinal Images Using Marker-controlled Watershed Transformation," *Springer, J Med. Syst.,* online Jan. 2010.

[2] A. Sopharak and B. Uyyanonvara, "Automatic Exudates Detection from Non-dilated Diabetic Retinopathy Retinal Images Using Fuzzy C-means Clustering," *Sensor*, vol. 9(3), pp. 2148-2161, 2009.

[3] M. Garcia, C. I. Sanchez, M. I. Lopez, D. Abasolo and R. Hornero, "Neural network basad detección of hard exudates in retinal images," *Computer Methods and Programs in Biomedicine*, vol. 93, pp. 9-19, 2009.

[4] D. Welfer, J Scharcanski and D. R. Marinho, "A coarse-to-fine strategy for automatically detecting exudates in color eye fundus images," *Computerized Medical Imaging and Graphics*, vol. 34, pp. 228-235, 2010.

[5] C. I. Sanchez, M. Garcia, A. Mayo, M. Lopez and R. Hornero, "Retinal image analysis based on mixture models to detect hard exudates," *Medical Image Analysis*, vol. 13, pp. 650-658, 2009.

[6] H. Li and O. Chutatape, "Automated feature extraction in color retinal images by a model based approach," *IEEE Trans. on Medical Engineering*, vol. 51, pp. 246-254, 2004.

[7] S. Sekhar, W. Al-Nuaimy and A. K. Nandi, "Automated Localization of Retinal Optic Disc Using Hough Transform," *ISBI 2008, France*, pp. 1577-1580, 2008.

[8] S. Sekhar, W. Al-Nuaimy and A. K. Nandi, "Automated Localization of Optic Disk and Fovea in Retinal Fundus Images" *EUSIPCO 2008*, Switzerland, 2008.

[9] H. F. Jaafar, A. K. Nandi and Waleed Al-Nuaimy, "Automated detection of exudates in retinal images using a split-and-merge algorithm," *EUSIPCO 2010*, Denmark, Alborg, pp. 1622-1626, 2010.

[10] S. Y. Chen, W. C. Lin and C. Chen, "Split-and-Merge Image Segmentation Based on Localized Feature Analysis and Statistical Test," *Graphical Models and Image Processing*, vol. 53(5), pp. 457-475, 1991.

[11] T. Kauppi *et al.*, "DIARETDB0: Evaluation database and morphology for diabetic retinopathy algorithm," *Technical report*, Lappeenranta University of Technology, Finland, 2006.

[12] T. Kauppi *et al.*, "DIARETDB1 diabetic retinopathy database and evaluation protocol," *Technical report,* Faculty of Medicine, University of Kuopio, Finland, 2007.

[13] T. Walter, J. C. Klein and P. Massin, "A Contribution of image processing to the diagnosis of diabetic retinopathy- detection of exudates in colour fundus images of the human retina," *IEEE Trans. Med. Imaging*, 21, pp. 1236-43, 2002.